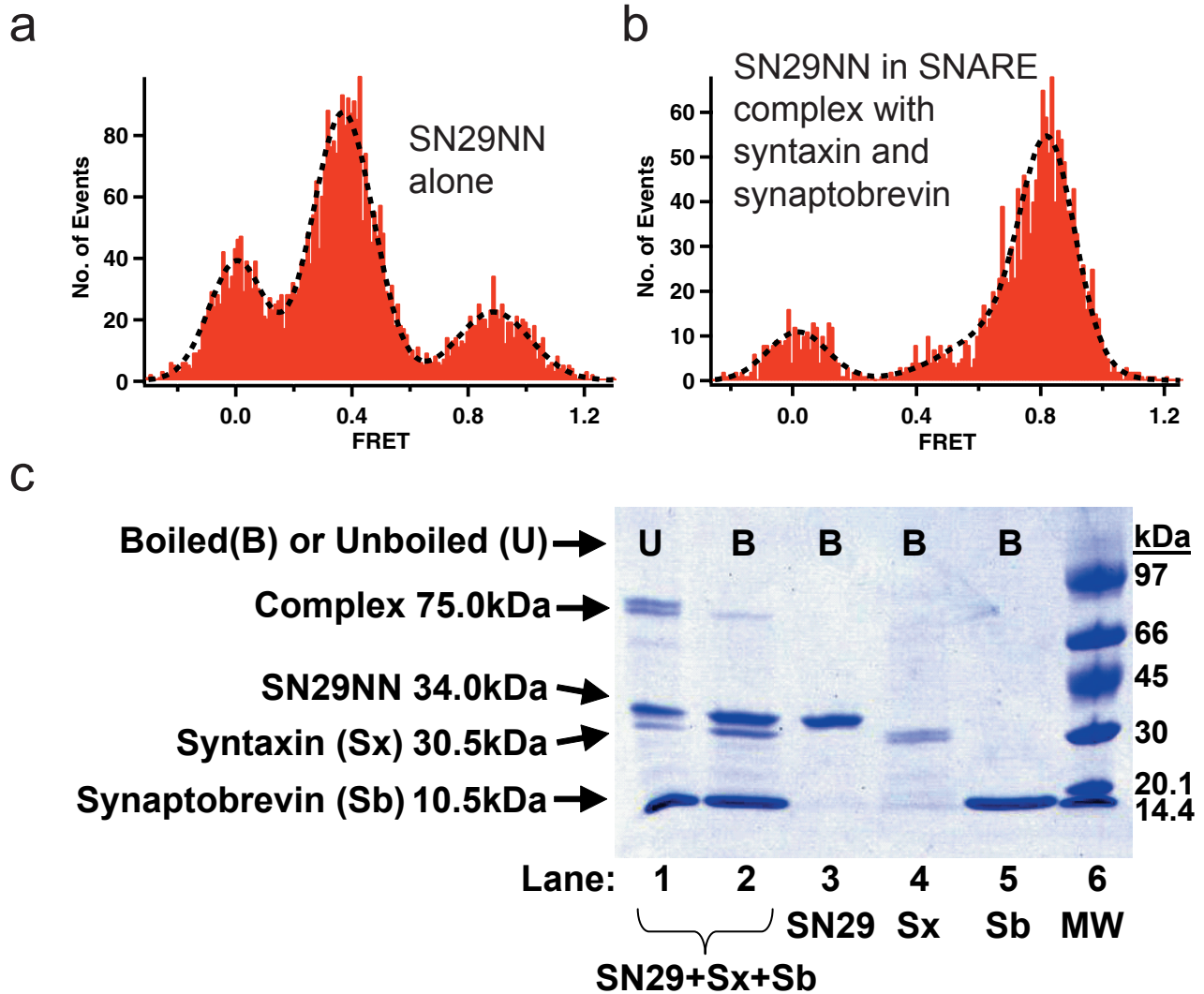
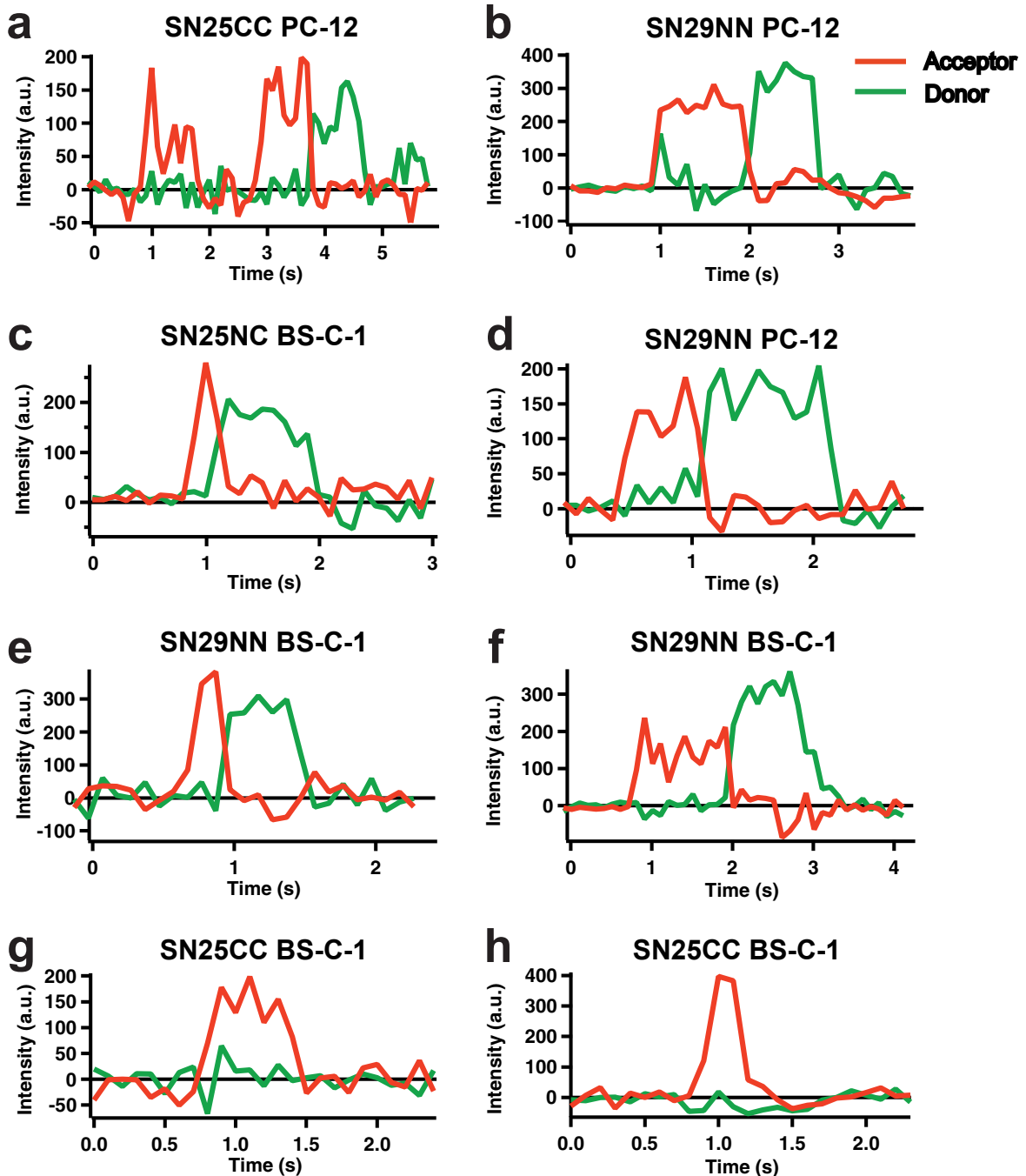


Supplementary Figure 1: Characterization of SN29NN.



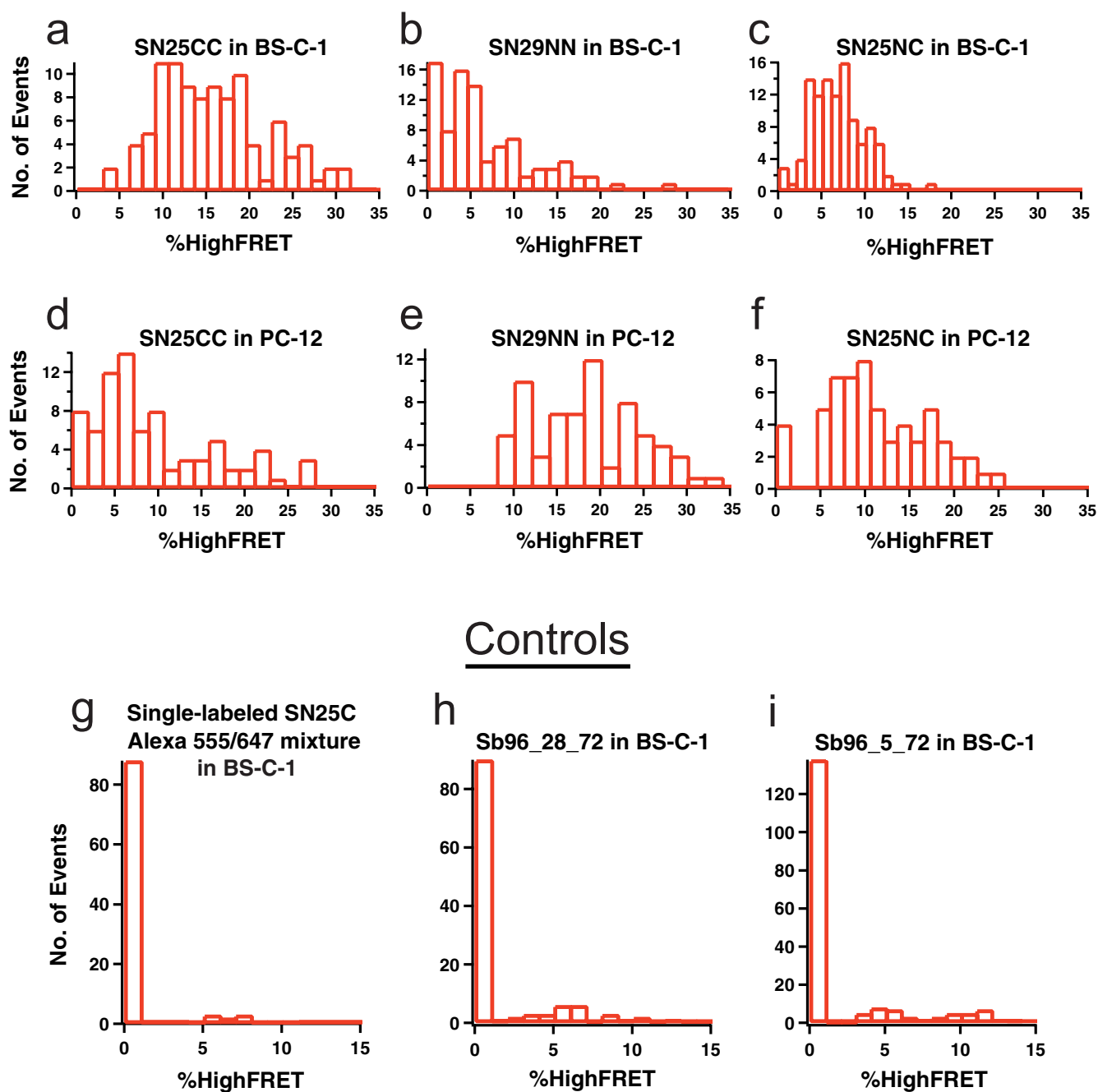
(a) SN29NN labeled with Alexa 555 and Alexa 647 was encapsulated inside liposomes tethered to a quartz surface and analyzed for single molecule FRET (online **methods**). The FRET distribution is dominated by a low FRET peak (0.37). A smaller FRET peak at 0.9 is likely due to protein aggregation. The FRET=0 peak is due to acceptor blinking and bleaching. (b) SN29NN labeled with Alexa 555 and Alexa 647 was assembled into SNARE complex with syntaxin and synaptobrevin and measured for smFRET as in **a**. The FRET peak revealed emission around 0.82. The SN29NN label sites are designed by alignment with SNAP-25 to give high FRET if the conformation is similar to that of SNAP-25 in the full SNARE complex. Thus the SN29NN label sites report entry into SNARE complex by a change from low FRET to high FRET. (c) SDS-PAGE (10–15% gradient phast gel with Coomassie staining; GE Biosciences) analysis reveals SNAP-29 forms an SDS resistant complex with syntaxin and synaptobrevin. Molecular weight markers are in lane 6 (Low molecular weight standards, GE Biosciences). Lanes 1 and 2 contain a mixture of SN29NN (unlabeled), syntaxin and synaptobrevin without boiling (lane 1) or with 5 minute boiling in SDS loading buffer (lane 2). Lanes 3-5 contain the individual protein samples (at the same final concentrations used in lanes 1 and 2) as indicated. An SDS-resistant complex with molecular weight between 66 and 97 kDa is visible in lane 1 that disappears upon boiling in lane 2.

Supplementary Figure 2: Additional examples of smFRET in cells.



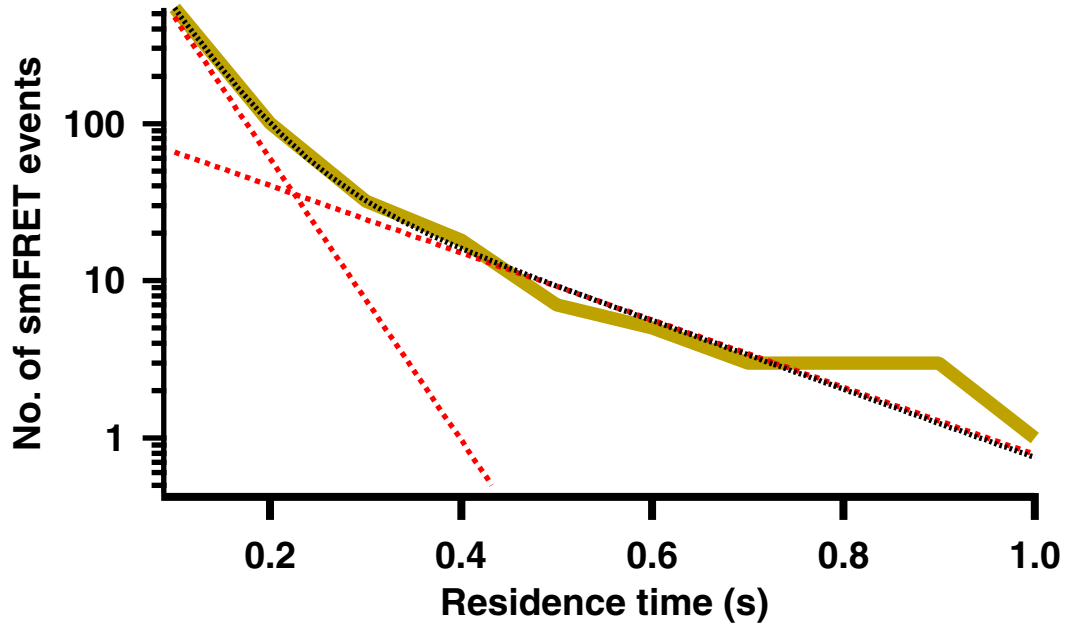
The protein and cell type is indicated above each graph. Acceptor emission is red and donor emission is green. (a-f) Traces selected to demonstrate anticorrelation of the donor and acceptor signals. (g-h) Common smFRET events where high acceptor emission is observed for the entire event indicating either donor bleaching or protein dissociation. For a and b, constant background values were derived from the average of acceptor and donor intensities for the 10 frames (1 second) after photobleaching during green illumination. For c-h, background was calculated by averaging intensity in the 16 pixels on the edge of a 5 pixel by 5 pixel region surrounding the 3 pixel by 3 pixel area centered on the imaged spot. All traces show acceptor and donor intensity values with their respective backgrounds subtracted. For b the green illumination was off for the first ten frames.

Supplementary Figure 3: Histograms of %HighFRET values.



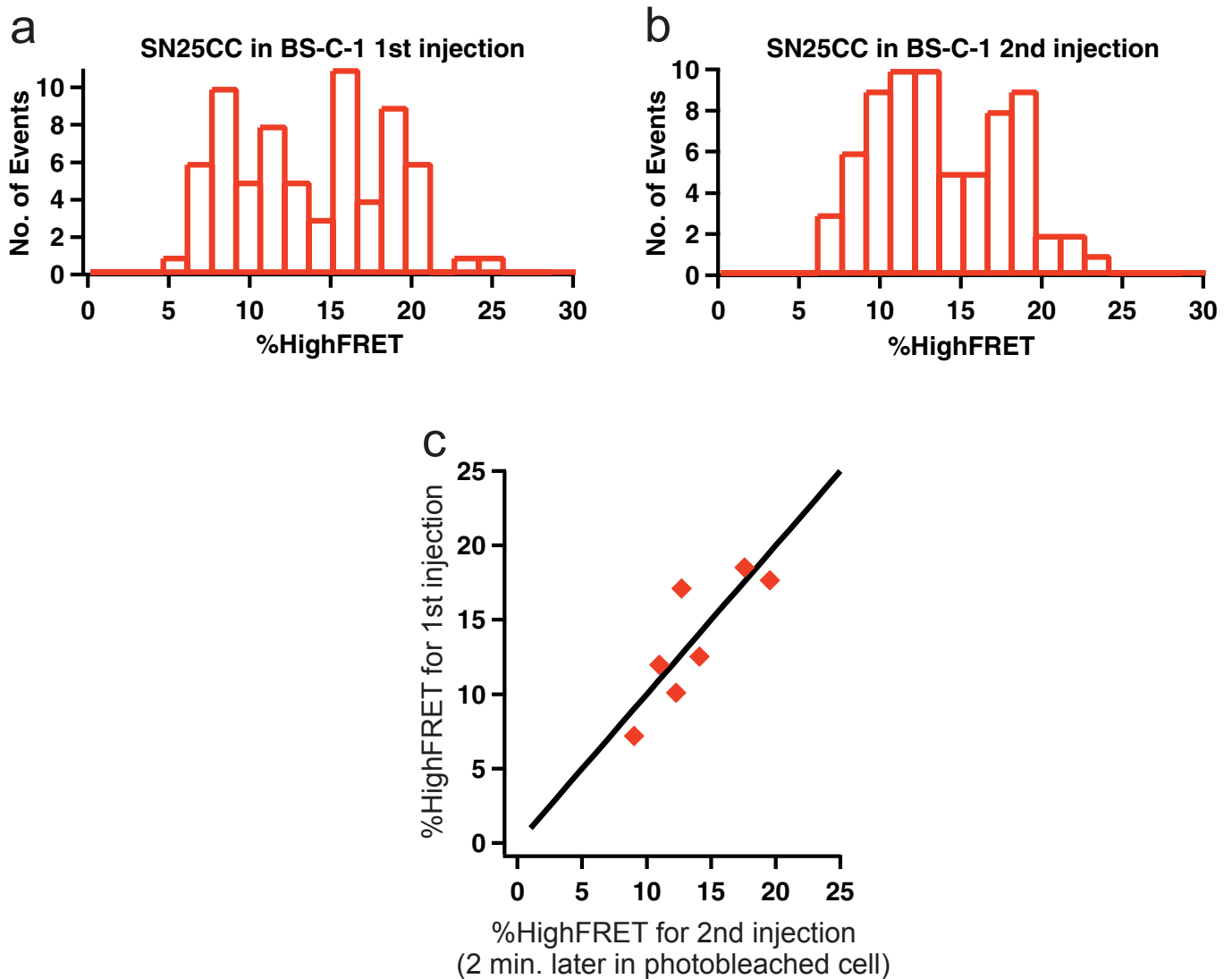
(a-i) Histograms of %HighFRET values (described in online **methods**) were accumulated from injections of different cells with the indicated protein and cell type. **Supplementary Table 1** reports the number of cells analyzed and averages for each of these graphs.

Supplementary Figure 4: Residence times of individual SN25CC membrane binding events in BS-C-1 cells.



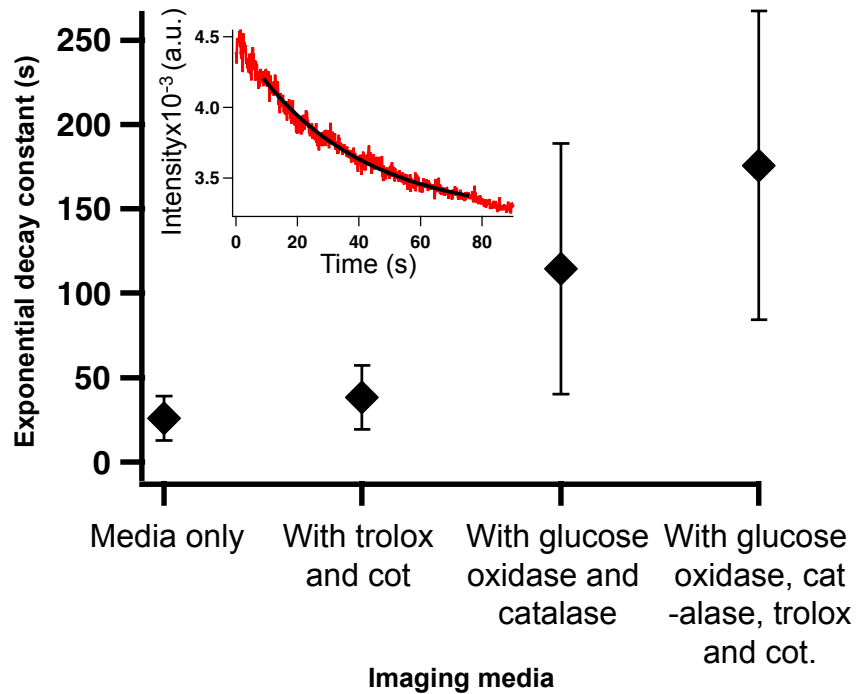
Dual-labeled SN25CC was microinjected into BS-C-1 cells and the residence time of each high smFRET event was measured. These were accumulated into a histogram and plotted on a semi-log graph. Single frame binding events were excluded when curve fitting. The dashed black line is a double exponential fit with 10% of the population having a decay constant of 0.2 seconds and 90% having a decay constant 0.05 seconds. The dashed red lines are single exponential fits with each of these time constants, demonstrating the appropriateness of the double exponential fit. Further details are in **Supplementary Note**.

Supplementary Figure 5: %HighFRET is unchanged for two sequential injections of a single cell before and after extensive photobleaching.



A single BS-C-1 cell was injected with SN25CC and ten %HighFRET values were calculated (online **methods**) for the first ten movie frames following the injection. The cell was then illuminated for two minutes with the green laser to bleach all of the injected dye-labeled protein and then a second, identical injection of the same cell was performed. The same analysis was performed after the second injection to generate ten %HighFRET values. **(a)** Histogram of the %HighFRET values for the first injection accumulated over seven different cells. **(b)** %HighFRET results for the second injection of these seven cells. The histogram is notably similar to **a**. The mean values (\pm one s.d.) of %HighFRET for the first and second injections are 13.6 ± 4.8 and 13.7 ± 4.2 . These values agree well with each other and with the data for SN25CC in BS-C-1 from other experiments (**Supplementary Table 1**). **(c)** Graph of the average of the ten %HighFRET values of the first injection of a cell plotted against the average of the ten %HighFRET values for the second injection of the same cell for the seven cells measured. The similarity of %HighFRET values for each cell before and after photobleaching confirms the similarity between the combined values in **a** and **b**.

Supplementary Figure 6: Effect of antioxidants and oxygen scavengers in media on *in vivo* microscopy.



The photobleaching time constant of fluorescent emission is shown for time courses of tracked, Alexa 647-labeled .1 μm polystyrene beads that were microinjected into BS-C-1 cells bathed in various additives (see online **methods**). The antioxidants trolox and cyclooctatetraene (cot) negligibly extended dye lifetimes while the oxygen scavenging system of glucose oxidase and catalase showed a strong improvement. The combination of these additives (right) had the longest time constant of all -- improving the dye lifetime by a factor of four. Background-corrected intensity time courses were fitted with an exponential decay function ($e^{-t/\tau}$; inset) and resulting time constant (τ) was averaged over multiple tracked beads (N=47, 80, 19 and 27 left to right on graph). Error bars show one s.d. of the average. Inset is an example of a raw (not background subtracted) intensity time course for a tracked bead in a cell.

Supplementary Table 1: %HighFRET values for combinations of proteins and cells.

Protein	Cell Type	Mean %HighFRET	N (cells)
SN25CC	BS-C-1	15.7±6.2	10
SN29NN	BS-C-1	6.4±5.7	9
SN25NC	BS-C-1	6.8±3.1	11
SN25CC	PC-12	9.5±7.8	8
SN29NN	PC-12	19.2±6.8	7
SN25NC	PC-12	11.2±5.9	6
<u>CONTROLS</u>			
Sb-NC_28_72	BS-C-1	1.7±3.5	12
Sb-NC_5_72	BS-C-1	2.0±4.0	19
Mixture of SN25C-donor-only & SN25C-acceptor-only	BS-C-1	0.9±2.4	10
SN25CC G43D	BS-C-1	1.0±2.5	10

Average values of %HighFRET (\pm one standard deviation) defined in online **methods** for the indicated combinations of protein and cell types. Histograms of the experiments used to form the averages are in **Fig. 2c-f** and **Supplementary Fig. 3**.

Supplementary Note

Single molecule analysis of the residence times of high FRET binding events

The residence time of an smFRET event is defined to be the number of consecutive frames in the same location displaying donor and acceptor intensities characteristic of high FRET. This is shown graphically in **Supplementary Figs. 2g-h**, where the residence times are ~ 1 and 0.5 s, respectively. Anticorrelated events, such as those seen in **Fig. 1d** and **Supplementary Fig. 2a-f**, were not included in these measurements as they report time until acceptor photobleaching and not protein dwell time. High smFRET events that terminate without anticorrelated donor recovery were indicative of the binding and unbinding of the microinjected protein within the cell. Donor photobleaching could also account for such terminating high FRET traces, however, in our system acceptors typically bleach faster than donors.

Residence times of smFRET for injection of SN25CC into multiple BS-C-1 cells were extracted from movies using custom software and accumulated into histograms. The resulting histograms required double exponential functions for accurate fitting (excluding the first bin) (**Supplementary Fig. 4**). We uncovered a fast binding state (0.05 s) less than our camera frame rate (100 ms) and a longer binding state (0.2 s) that occurred in ~ 10 % of events. Similar double exponentials were required for fitting of all residence time histograms of all microinjected protein types. The longer-lived state is likely limited by dye lifetimes before photobleaching.

Single particle tracking of mobile events

We performed single particle tracking of high smFRET emitting proteins using standard methods¹ (**Fig. 2b**). The coordinates of the center of the diffraction limited spot recorded for molecules with high smFRET were used to analyze mobility by finding Δr over each Δt , (100 msec frame rate), solving for $D = \Delta r^2/4\Delta t$ and averaging these values. The average of 10 stationary particles yielded a noise limited resolving floor value of $D = 0.045 \pm 0.016 \mu\text{m}^2 \text{s}^{-1}$. FRET efficiency histograms for tracked single molecules were similarly bimodal with peaks around 0 and 1, as in **Fig. 1e**.

While the vast majority of high smFRET events did not move in the x-y plane, ~ 3.5 % exhibited diffusive motion inside the cell greater than our noise detection limit. For SN25CC in BS-C-1 cells the average D for 5 tracked, mobile molecules was $D = 0.266 \pm 0.052 \mu\text{m}^2 \text{s}^{-1}$. Successful microinjection was confirmed as protein molecules outside the cell diffused with D values over an order of magnitude higher.

References:

1. Saxton, M.J. and Jacobson, K. *Annu. Rev. Biophys.*, **26**, 373-399 (1997).